Light propagation in optical crystal powders: effects of particle size and volume filling factor

2007 J. Phys.: Condens. Matter 19 456213

(http://iopscience.iop.org/0953-8984/19/45/456213)

IOP PUBLISHING JOURNAL OF PHYSICS: CONDENSED MATTER

J. Phys.: Condens. Matter **19** (2007) 456213 (13pp) doi:10.1088/0953-8984/19/45/456213

Light propagation in optical crystal powders: effects of particle size and volume filling factor

B García-Ramiro[1], M A Illarramendi[1], I Aramburu[1], J Fernández[1,2,3], R Balda[1,2,3] and M Al-Saleh[1]

[1] Departamento de Física Aplicada I, Escuela Técnica Superior de Ingeniería, Universidad del País Vasco, Alameda Urquijo s/n, 48013 Bilbao, Spain
[2] Unidad Física de Materiales CSIC-UPV/EHU, 20080 Donostia, Basque Country, Spain
[3] Donostia International Physics Center (DIPC), 20080 Donostia, Basque Country, Spain

E-mail: mepgarab@ehu.es (B García-Ramiro)

Received 2 August 2007
Published 15 October 2007
Online at stacks.iop.org/JPhysCM/19/456213

Abstract

In this work, we analyse the light propagation in some laser and nonlinear crystal powders. In particular, we study the dependence of the diffusive absorption lengths and the transport lengths on particle size and volume filling factor. The theoretical calculations have been made by assuming a diffusive propagation of light in these materials.

1. Introduction

Random lasers, in which gain is combined with multiple scattering of light, are being actively investigated [1–7]. The laser radiation generated in laser crystal powders (LCP) is usually described as random lasing with nonresonant feedback where the central emission wavelength of such a laser is determined by the resonant wavelength of a gain medium rather than eigenmodes of the cavity. This type of laser has no spatial coherence, it is not stable in phase, and its photon statistics are strongly different from that of a conventional laser. Consequently, laser crystal powders are attractive as compact and mirrorless lasers where the coherence is not necessary or the absence of coherence is desirable. These characteristics can be advantageous in holography, in laser inertial confinement fusion or in transport of energy in fibers for medical applications [8]. The potential applications of LCP motivate the study of their optical properties and the search for new crystal powder materials. This is the case of Nd^{3+}-doped potassium lead chloride crystals (KPb_2Cl_5) or potassium bismuth/neodymium molybdate crystals ($K_5Bi_{1-x}Nd_x(MoO_4)_4$).

KPb_2Cl_5 crystals have recently attracted much attention because they are nonhygroscopic, chemically stable, have a large transparency window (0.3–20 μm) and a highest phonon energy of about 203 cm^{-1}. A host with low phonon energy leads to low nonradiative transition rates due to multiphonon relaxation and high radiative transitions rates, which increase the

quantum efficiency from the excited states of active ions. The spectroscopic properties of $KPb_2Cl_5:Nd^{3+}$ have been investigated, showing that laser action up to 9 μm should be possible in this material [9–11]. Among oxide laser crystals with a disordered structure, palmierite-type $K_5Bi_{1-x}Nd_x(MoO_4)_4$ compounds have generated a great interest as potential laser materials [12–15]. The lasing wavelength range of these materials is confined within the 1063–1070 nm region.

On the other hand, second harmonic generation measurements on powders of nonlinear optical crystals have been used to determine the average value of nonlinear optical coefficients [16]. These values are usually given relative to that of a nonlinear optical crystal of well known properties used as a reference, such as the KH_2PO_4 crystal [17].

In order to better understand the operation regime of random lasers or the generation of the second harmonic in powders, a detailed characterization of light propagation in these scattering materials is needed. In particular, the knowledge of the mean-free-path lengths involved in the scattering and absorption processes that take place in these materials together with their dependence on the characteristic parameters of the sample (particle size and volume filling factor) are very important to analyse the behavior of these optical systems. For instance, it has been shown that the threshold of random lasers is strongly dependent on the transport mean-free-path [18–20]. On the other hand, the scattering of light by powders of nonlinear crystals, characterized by the scattering lengths, plays an important role in the second harmonic generation, decreasing the efficiency and making more difficult the analysis and interpretation of the second harmonic radiation generated by the sample. In the present work we have determined the diffusive absorption lengths and the transport lengths in $KPb_2Cl_5:Nd^{3+}$ and KH_2PO_4 crystal powders by using reflectance and transmittance measurements. Moreover, we have analysed the dependence of these lengths on particle size (in KH_2PO_4 powders) and on the volume filling factor (in $K_5Bi_{0.9}Nd_{0.1}(MoO_4)_4$ powders).

The paper is organized as follows. The experimental techniques are described in section 2. The theoretical analysis of the diffuse reflectance and transmittance of crystal powders under a diffusion assumption is analysed in section 3. In section 4, the scattering and absorption lengths of some crystal powders are calculated and the obtained results are discussed. The summary of the work is presented in section 5.

2. Experimental details

In our experiments, we have used ground powders of $KPb_2Cl_5:Nd^{3+}(1\%)$ (KPC) and $K_5Bi_{0.9}Nd_{0.1}(MoO_4)_4$ (KBNM) laser crystals. Details of the crystallographic structure of their single crystals and their laser properties have been previously reported by some of the authors [11, 13, 21]. We have also studied ground powders of KH_2PO_4 (KDP) nonlinear crystals. The crystalline powder with a mean particle size of 50 μm and 99.999% pure was obtained from Alfa Caesar, Inc.

The polydispersity of the measured powders was evaluated from SEM (scanning electron microscope) photographs like the one shown in figure 1. The particle size has been computed calculating the mean of the major and minor axis lengths of the grains. As an example, figure 2 shows the histogram of the particle size corresponding to the laser crystal powder $KPb_2Cl_5:Nd^{3+}$ (1%). By fitting the histograms to a log-normal function we obtain the average particle size and its standard deviation. The volume filling factor of the powder materials (f) has been calculated by measuring volume and weight of the samples. The characteristics of the studied powders are displayed in table 1.

The diffuse reflectance and transmittance spectra of the powders were recorded by use of a Cary 5 spectrophotometer with an integrating sphere assembly. The samples were

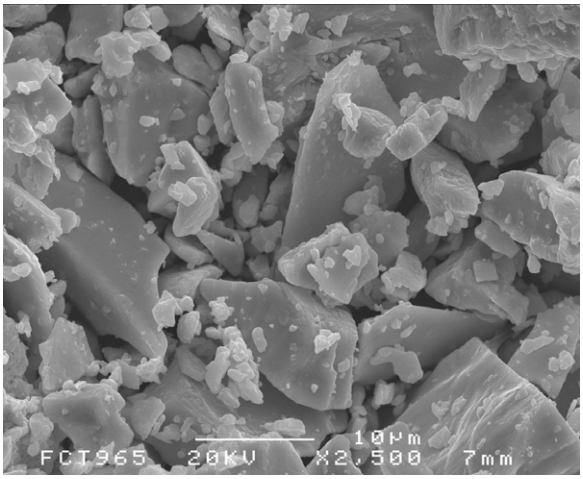

Figure 1. Scanning electron microscope photograph of the laser crystal $KPb_2Cl_5:Nd^{3+}$ (1%) particles.

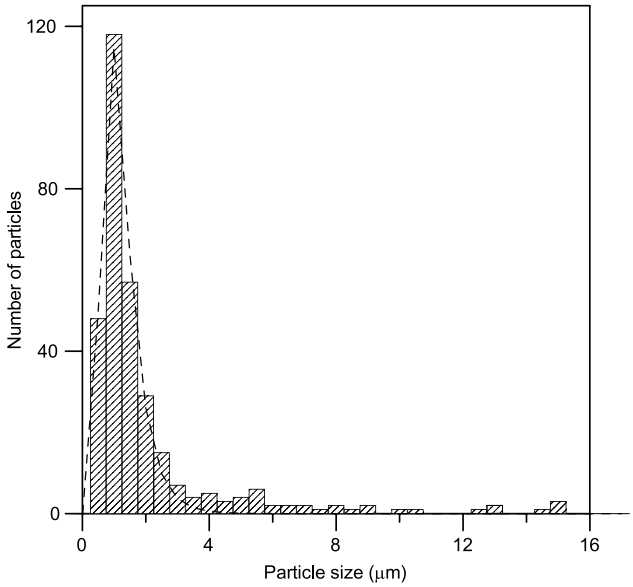

Figure 2. Histogram of the KPC particle size. The dashed line is the log-normal fit from which the average particle size is calculated.

attached to the rear or the front port of the integrating sphere, depending on the measurement performed (see figure 3). The appropriate normalizations of the recorded spectra have been made to the reflection/transmission of the diffused ideally white standard reference samples. The transmission measurements of the samples at high thickness (from $L = 1000$ μm) were acquired using a narrow-angle arrangement. The incoming light beam, an Ar laser, was perpendicularly incident onto the sample. The transmitted signal was collected with a Hamamatsu R928 photomultiplier in a narrow solid angle at the direction of the incoming light beam. The signal was amplified by a standard lock-in technique. The room temperature

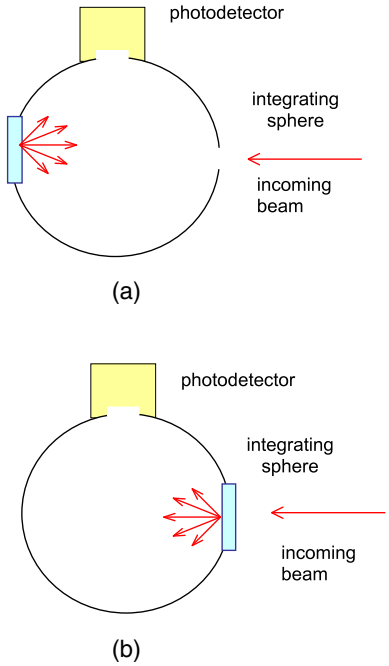

Figure 3. Integrating sphere setup. (a) Diffuse reflection spectra collection. (b) Diffuse transmission spectra collection.

(This figure is in colour only in the electronic version)

Table 1. Characteristics of the studied powders. The ratio between the standard deviation and the average particle size gives the polydispersity of the powders. It is around 50% in almost all samples.

Material sample	Particle size (μm)	Volume filling factor
KPb_2Cl_5:Nd^{3+} (1%) (KPC)	1.2 ± 0.6	0.55 ± 0.05
KH_2PO_4 (KDP)	50 ± 25	0.55 ± 0.05
	30 ± 15	
	15 ± 7	
	9 ± 5	
	4.5 ± 2	
$K_5Bi_{0.9}Nd_{0.1}(MoO_4)_4$ (KBNM)	2.4 ± 0.8	0.50 ± 0.05
		0.55 ± 0.05
		0.58 ± 0.05
		0.60 ± 0.05

absorption spectra of the single crystals in the 300–850 nm spectral range were recorded by the Cary 5 spectrophotometer.

3. Theory

Light propagation through optically dense random systems, where the transport mean-free-path is much longer than the light wavelength ($l_t \gg \lambda$), is commonly described in terms of a

diffusion equation. In one dimension the stationary diffusion equation is written as:

$$0 = \frac{\partial^2 U_\mathrm{d}}{\partial^2 z} - \frac{U_\mathrm{d}}{l_\mathrm{abs}^2} + p(z), \tag{1}$$

where $U_\mathrm{d}(z)$ is the average diffuse intensity, $l_\mathrm{abs} = \sqrt{\frac{l_\mathrm{t} l_\mathrm{i}}{3}}$ is the diffusive absorption length and $p(z)$ is the source of diffuse radiation. In this case, the source is the light incoming onto the sample in the z direction which is extinguished (scattered and absorbed) along the scattering sample. The definitions of the mean-free-path lengths involved in the scattering and absorption processes are given in the appendix. As in other works [22–24], we have replaced the incoming light beam at the boundary by a source of diffuse radiation located at a certain plane inside the sample. In order to make this plane source equivalent to the real one, we have calculated the average position wherein the incident energy is introduced in the sample. On account of the incoming light decaying exponentially through the slab as, $J_0 \exp(-\frac{z}{l^*})$, the average position is calculated by:

$$\bar{l} = \frac{\int_0^L z J_0 \exp(-z/l^*)\,\mathrm{d}z}{\int_0^L J_0 \exp(-z/l^*)\,\mathrm{d}z} = l^* - \frac{L}{\exp(L/l^*) - 1}, \tag{2}$$

where l^* is the extinction mean-free-path, J_0 is the incident flux and L is the sample thickness. Due to $L \gg l^*$, we get $\bar{l} = l^*$. Therefore, we assume that the incident photons are left inside the sample at the position $z = l^*$ and express the source as $p(z) = J_0 \delta(z - l^*)$. For a slab geometry oriented in the x–y plane, the boundary conditions of equation (1) are determined by considering that the diffuse fluxes going from the borders ($z = 0$ and L) inside the sample are due to the internal reflectivities at the sample surfaces (r). In the limit of weakly absorbing samples, these conditions are equivalent to those obtained by extrapolating U_d to 0 at a distance l_e outside the sample surface, that is, $U_\mathrm{d}(-l_\mathrm{e}) = U_\mathrm{d}(L + l_\mathrm{e}) = 0$ [25]. Taking into account the internal reflectivities at the sample surfaces, the extrapolation length (l_e) is given by $l_\mathrm{e} = \frac{2h}{3} l_\mathrm{t}$, where $h = \frac{1+r}{1-r}$, and l_t is the transport mean-free-path.

The diffuse reflectance R of the slab has been calculated by the diffuse flux evaluated at the sample surface $z = 0$ and normalized by the incident flux (J_0) whereas the transmittance T is due to the normalized diffuse flux evaluated at the sample surface $z = L$. The obtained expressions for these magnitudes are written as:

$$R = \cosh\left(\frac{l_\mathrm{e}}{l_\mathrm{abs}}\right) \frac{\sinh\left(\frac{L + l_\mathrm{e} + l^*}{l_\mathrm{abs}}\right)}{\sinh\left(\frac{L + 2l_\mathrm{e}}{l_\mathrm{abs}}\right)} \tag{3}$$

$$T = \frac{1}{2}\left(\frac{\sinh\left(\frac{l^*}{l_\mathrm{abs}}\right) + \sinh\left(\frac{l^* + 2l_\mathrm{e}}{l_\mathrm{abs}}\right)}{\sinh\left(\frac{L + 2l_\mathrm{e}}{l_\mathrm{abs}}\right)}\right). \tag{4}$$

At large values of L ($L \gg l_\mathrm{abs}$) the reflectance does not depend on sample thickness and it can be written very simply as:

$$R = \frac{1}{2}\left(1 + \exp\left(\frac{-2l_\mathrm{e}}{l_\mathrm{abs}}\right)\right). \tag{5}$$

On the other hand, when $L \gg l_\mathrm{abs}$ the transmittance decays exponentially with thickness and if $l_\mathrm{abs} \gg l^*$ (low absorption) it can be expressed as:

$$T = T_0 \exp\left(\frac{-L}{l_\mathrm{abs}}\right) \qquad \text{with } T_0 = \sinh\left(\frac{2l_\mathrm{e}}{l_\mathrm{abs}}\right) \exp\left(\frac{-2l_\mathrm{e}}{l_\mathrm{abs}}\right). \tag{6}$$

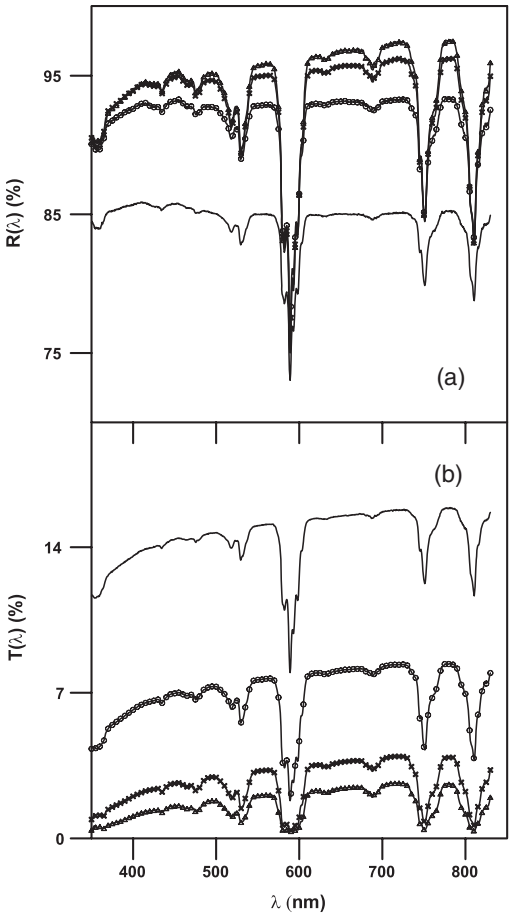

Figure 4. (a) Spectral diffuse reflectance and (b) spectral diffuse transmittance of $KPb_2Cl_5:Nd^{3+}$ (1%) powders. Solid line corresponds to a sample thickness $L = 100$ μm, solid line with dots to $L = 200$ μm, solid line with crosses to $L = 500$ μm and solid line with triangles to $L = 750$ μm. The same nomenclature has been used in both sections of the figure. The volume filling factor of the powder materials in these measurements is $f = 0.55 \pm 0.05$.

4. Results and discussion

4.1. Calculation of the transport mean-free-paths in KPC powders

The diffuse reflectance and transmittance curves of the KPC sample in the 350–830 nm spectral range have been plotted in figure 4 for several sample thickness. All curves have been recorded using an integrated sphere and correspond to absolute measurements. As follows from the figure, Nd absorption is practically absent in some spectral ranges. The dependence on the sample thickness of the diffuse reflectance and transmittance, R and T, at several wavelengths is shown respectively in figures 5 and 6. One can see in these figures that the diffuse reflectance is nearly constant and the diffuse transmission decreases exponentially with the sample thickness at $L \geqslant 500$ μm. By fitting the experimental points of figure 6 to equation (6) we determine the constant of the exponent, l_{abs}, and the intersection of the straight line and the vertical axis, T_0. The obtained values for l_{abs} and T_0 at $\lambda = 457$, 465, 477, 488, 496,

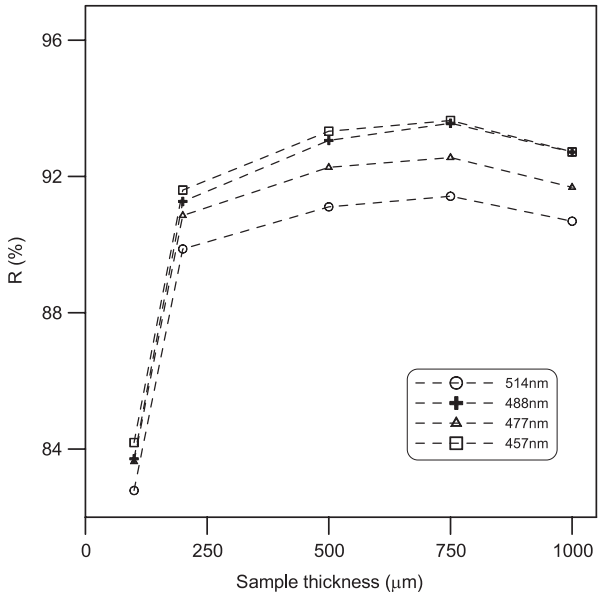

Figure 5. Diffuse reflectance of $KPb_2Cl_5:Nd^{3+}$ (1%) compound as a function of the sample thickness. (○) λ = 514 nm, (+) λ = 488 nm, (△) λ = 477 nm, (□) λ = 457 nm. The symbols represent the experimental points and the dashed lines are a guide for the eye.

Table 2. Absorption coefficient (k_{abs}) of KPC crystal. Diffusive absorption lengths l_{abs}, T_0 values, and transport mean-free-paths l_t of KPC powders at several wavelengths determined from the results of the transmission measurements.

	λ (nm)					
	457	465	477	488	496	514
k_{abs} (cm^{-1}) in bulk KPC	∼0	0.01	0.02	0.002	∼0	0.04
l_{abs} (μm)	343 ± 19	297 ± 6	264 ± 12	303 ± 21	309 ± 8	227 ± 10
T_0	8.9 ± 2	13.6 ± 1.5	15.3 ± 4	11.1 ± 3	10.3 ± 1	23.4 ± 5
l_t (μm) determined from T_0	3.2 ± 0.9	4.5 ± 0.7	4.6 ± 1.7	3.6 ± 1.3	3.4 ± 0.5	6.9 ± 2.3

and 514 nm are displayed in table 2. This table also shows the absorption coefficients of a KPb_2Cl_5 crystal at neodymium concentration equal to 1% at those wavelengths. An increase of absorption coefficient (k_{abs}) must imply a reduction of l_{abs} due to the shortening of l_i. This dependence of l_{abs} with absorption can be observed in the table where the measured values for l_{abs} at very low-absorbing spectral range (457, 488, and 496 nm) are larger than the values measured at the other wavelengths where the absorption is higher.

Once the values of l_{abs} and T_0 have been calculated, we can estimate the transport mean-free-paths by using the expression of T_0 displayed in equation (6) [26]. In these calculations we have used $h = 7.76$ corresponding to the internal reflectivity r equal to 77%. The internal reflectance of the sample has been estimated from the Fresnel equations [27] by using the real part of the refractive index of both the sample material ($n = 2.019$) and the cuvette where the sample was placed ($n = 1.5$). The obtained values for l_t at the studied wavelengths have been included in table 2. One can see that the values of l_t in the low-absorbing spectral region (457, 488, and 496 nm) are in a good agreement with each other and practically independent of the light wavelength. A weak wavelength-dependence of light scattering takes place when particle

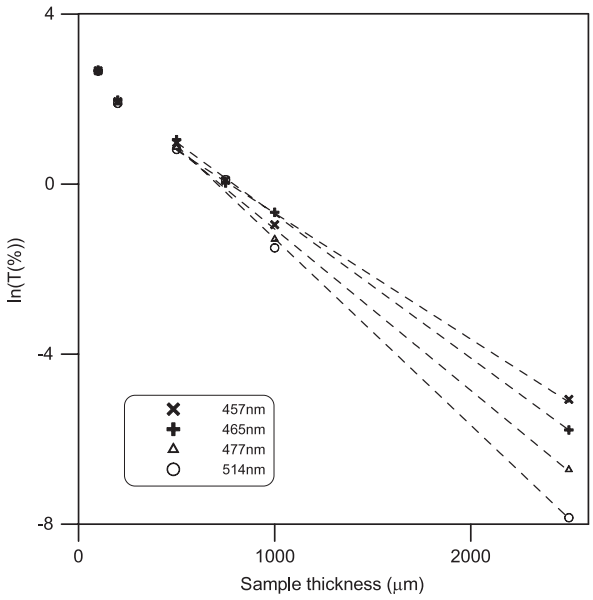

Figure 6. Transmittance of $KPb_2Cl_5:Nd^{3+}$ (1%) compound as a function of the sample thickness. (×) λ = 457 nm, (+) λ = 465 nm, (△) λ = 477 nm, (○) λ = 514 nm. The symbols represent the experimental points and the dashed lines are the linear fitting. The coefficient of determination (R^2) of all the linear fittings is 0.99.

size is larger than the wavelength. The transport mean-free-paths at higher absorbing region (465, 477, and 514 nm) are somewhat larger than the previously calculated ones. Theoretically, they should be smaller. This discrepancy can be explained by taking into account the fact that the applicability of equation (6) requires $l_{abs} \gg l^*$, which is better verified when the absorption is nearly negligible.

We can also calculate the transport mean-free-paths by using equation (5) and the values of diffuse reflectance R at large sample thickness. Figure 7 shows the variation of $\ln(2R-1)$ with $1/(l_{abs})$. The l_{abs} values are those shown in table 2. By assuming that the transport mean-free-paths (and therefore the extrapolation length) do not vary in the studied spectral range (457–514 nm), the fitting of the experimental points of figure 7 to equation (5) gives directly the value of the extrapolation length in that range. The obtained value for l_e is 17.4 ± 2.9 μm and from this, we obtain the value for l_t, $l_t = 3.3 \pm 0.6$ μm. Taking into account the estimated errors we can say that this value of l_t agrees with those obtained from the values of T_0 at the low absorbing range. This result confirms the applicability of equation (6) under low absorption conditions.

4.2. Dependence on particle size of the diffusive absorption lengths in KDP powders

Figure 8 shows the dependence on particle size (ϕ) of the Neperian logarithm of the transmission measurements of KDP powders at fixed sample thickness ($L = 5000$ μm). From equation (6), the Neperian logarithm of the transmitted signal, $\ln(T)$, is given by $\ln(T) = \ln(T_0) - L/l_{abs}$ with $l_{abs} = \sqrt{\frac{l_i l_t}{3}}$. If we assume that the inelastic mean-free-path l_i does not depend on particle size whereas the transport mean-free-path depends linearly on

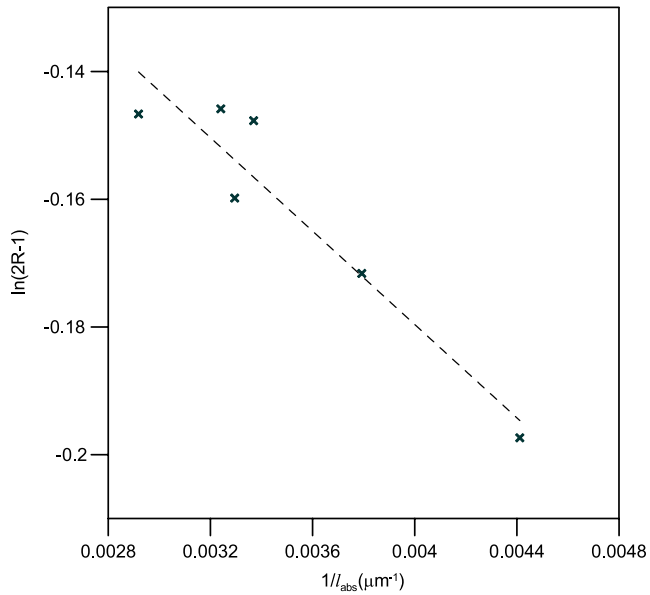

Figure 7. $\ln(2R-1)$ as a function of $1/l_{\mathrm{abs}}$. The symbols represent the experimental points and the solid line is the fitting to equation (5). The coefficient of determination (R^2) of the fitting is 0.90.

it [28], we can express the variation of $\ln(T)$ with particle size as:

$$\ln(T) = \ln(T_0) - \frac{L}{l_{\mathrm{abs}}} = \ln(T_0) - \frac{L}{\sqrt{\frac{l_t l_i}{3}}} = \ln(T_0) - \frac{L}{\sqrt{\frac{K l_i}{3}}}\phi^{-\frac{1}{2}} \qquad \text{with } l_t = K\phi. \tag{7}$$

Although it is not explicitly indicated in the equation, $\ln(T_0)$ also depends on particle size. However, if the sample thickness is sufficiently large, it can be demonstrated that the variation of $\ln(T_0)$ with respect to ϕ is much lower than the variation of L/l_{abs}. The dashed line plotted in figure 8 is the fit of the experimental points to equation (7) with T_0 constant. It can be seen that the obtained fit is reasonably good, indicating that the assumed dependences of the lengths on particle size can be considered correct. Moreover, the value of the parameter obtained from the fit $\frac{L}{\sqrt{\frac{K l_i}{3}}} = 16.3 \pm 1.8\ \mu\mathrm{m}^{1/2}$ can be used to obtain the value of l_{abs} as a function of particle size: $l_{\mathrm{abs}} = \frac{L}{16.3}\phi^{\frac{1}{2}}$ with $L = 5000\ \mu$m. The obtained values for l_{abs} using this expression are displayed in table 3.

The transmittance as a function of the sample thickness for several KDP powders of different particle size is plotted in figure 9. These measurements can be fitted to equation (6) in order to obtain the values of l_{abs} and T_0 and from these, the transport mean-free-paths. The obtained values for l_{abs} and T_0 as a function of particle size of KDP powders, in addition to the calculated value for l_t, have been included in table 3. For these samples we have used $h = 3.6$, corresponding to the internal reflectivity r equal to 56%. As in the potassium lead chloride compounds, the internal reflectance of the sample has been estimated by using the real part of the refractive index of both the sample material ($n = 1.49$) and the cuvette where the sample was placed ($n = 1.5$) [27]. It can be observed that good agreement between the values of l_{abs} is obtained from figure 8 and from figure 9. The first points of the fit to equation (6) in figure 9 correspond to a sample thickness $L = 1000\ \mu$m which is comparable with l_{abs} (see table 3). Consequently, the exponential dependence of transmittance could not be

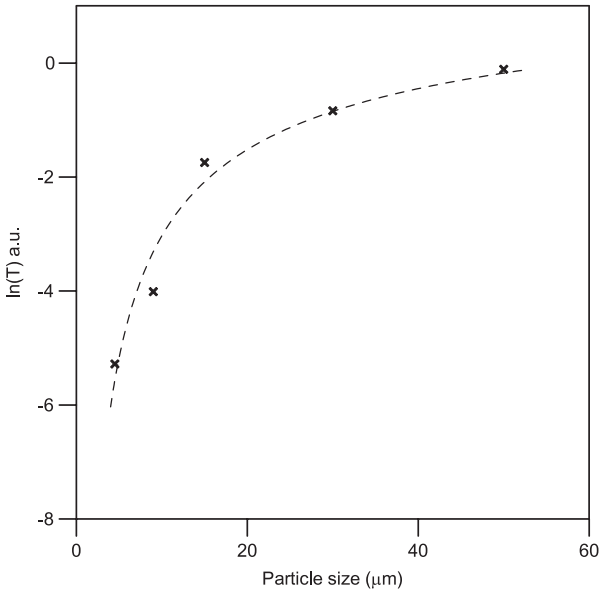

Figure 8. $\ln(T)$ as a function of particle size corresponding to the KDP compound. The symbols represent the experimental points and the dashed line is the fitting to the equation (7). The coefficient of determination (R^2) of the fitting is 0.96. The measurements have been acquired at $\lambda = 514$ nm with a sample thickness $L = 5000$ μm. The volume filling factor of the powder materials is $f = 0.55 \pm 0.05$.

Table 3. Diffusive absorption lengths l_{abs}, T_0 values, and transport mean-free-paths l_t as a function of particle size of KDP powders. The value of T_0 for the sample with $\phi = 30$ μm, (and therefore the value of l_t) has not been displayed because the absolute transmitted signal could not be measured. The values in the last row correspond to the values of l_t obtained by Mie theory in the independent scattering approximation.

	ϕ (μm)			
	4.5	9	15	30
l_{abs} (μm) from figure 8	649 ± 63	918 ± 52	1185 ± 36	1676 ± 26
l_{abs} (μm) from figure 9	695 ± 70	866 ± 92	1086 ± 141	1250 ± 150
T_0	7.8 ± 3.7	9.3 ± 3.7	18.3 ± 7.2	—
l_t (μm)	12.3 ± 7.6	18.6 ± 10.2	51.7 ± 32.5	—
l_t (μm) (Mie theory)	10.8	25.2	45.8	

satisfied for that sample thickness. However, the experimental results suggest that in practice, the applicability range of the exponential dependence of transmittance can be extended from $L \gg l_{abs}$ to $L \sim l_{abs}$. With regard to the transport lengths, the obtained values agree within the experimental error with those calculated from the Mie theory in the independent scattering approximation (see table 3).

4.3. Dependence with volume filling factor of the diffusive absorption lengths in KBNM powders

We now analyse the variation of the light propagation with the volume filling factor (f). In a previous paper [29], the authors showed that the transport mean-free-paths of molybdate

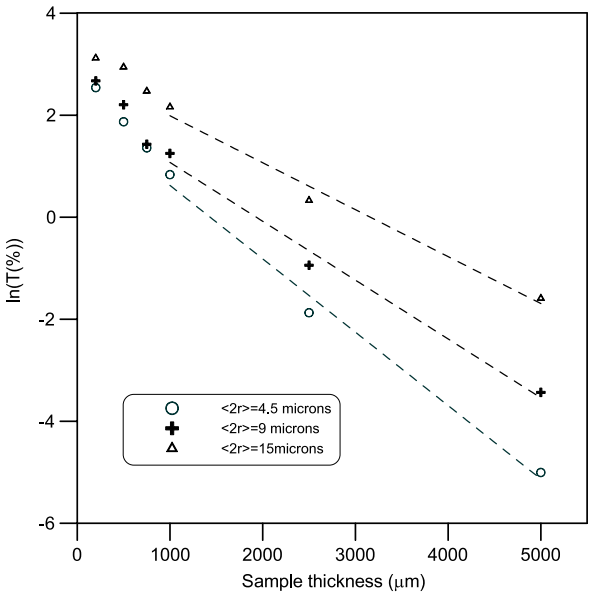

Figure 9. Transmittance for different particle sizes of the KDP compound as a function of the sample thickness. (○) $\phi = 4.5\ \mu$m, (+) $\phi = 9\ \mu$m, (△) $\phi = 15\ \mu$m. The symbols represent the experimental points and the dashed lines are the linear fitting. The coefficients of determination (R^2) of the linear fittings vary from 0.98 to 0.99. The measurements have been acquired at $\lambda = 514$ nm and the volume filling factor of the powder materials is $f = 0.55 \pm 0.05$.

crystal powders with high f (closely packed powders) would not basically change if spatial correlations were taken into account. That is, the scattering between particles could be considered independent. In the independent scatterer approximation, the scattering and absorption lengths are inversely proportional to f [28]. In this case, the diffusive absorption length l_{abs} would be expressed as $l_{\text{abs}} = \frac{K'}{f}$ and consequently $\ln(T)$ would be written:

$$\ln(T) = \ln(T_0) - \frac{L}{K'} f. \tag{8}$$

Although $\ln(T_0)$ also depends on f, it can be demonstrated that the variation of $\ln(T_0)$ with respect to f is much lower than the derivative of L/l_{abs} if the sample thickness is large. Figure 10 shows the variation of $\ln(T)$ in KBNM powders at $\lambda = 488$ nm as a function of the volume filling factor with a fixed sample thickness ($L = 4000\ \mu$m). The solid line is the fit of experimental points to equation (8). As follows from the figure, we can say that the assumption of independent scattering can be considered correct. From the parameter obtained from the fit, $L/K' = 20.4 \pm 1.6$, we can estimate the values for l_{abs} as a function of f: $l_{\text{abs}} = L/(20.4f)$ with $L = 4000\ \mu$m, which gives $l_{\text{abs}} = 326 \pm 50\ \mu$m for $f = 0.6$. This result is in good agreement, within the expected error range, with the value of l_{abs} obtained for molybdate crystal powders without neodymium ($K_5Bi(MoO_4)_4$) under the same conditions ($l_{\text{abs}} \sim 200\ \mu$m) [29].

5. Summary

(a) We have experimentally determined the transport mean-free-paths in KPb_2Cl_5:Nd^{3+} (1%) laser crystal powder in the 457–514 nm wavelength range by using diffuse reflectance and transmittance measurements.

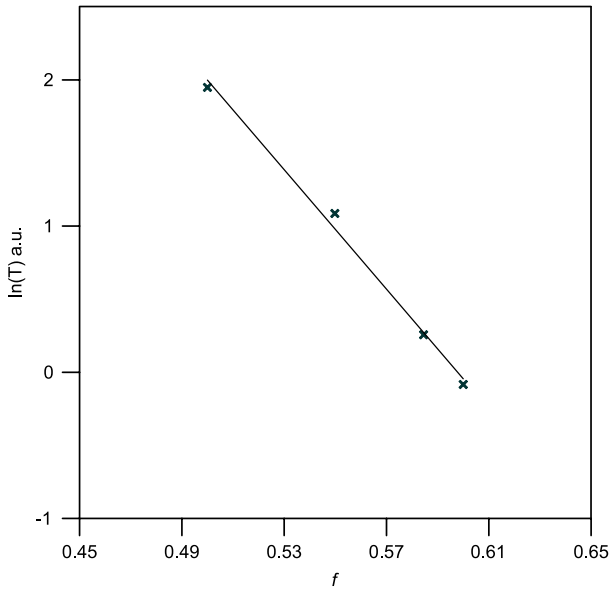

Figure 10. $\ln(T)$ as a function of the volume filling factor f corresponding to the KBNM sample. The symbols represent the experimental points and the solid line is the fitting to equation (8). The coefficient of determination (R^2) of the linear fitting is 0.99. The measurements have been acquired at $\lambda = 488$ nm with a sample thickness $L = 4000$ μm. The average particle size of the powders is $\phi = 2.4 \pm 0.8$ μm.

(b) The dependence on particle size of the diffusive absorption lengths of KH_2PO_4 crystal powders has been analysed. Good agreement between the experimental measurements and the theoretical predictions has been obtained, assuming that l_{abs} varies with the squared root of the particle size ($\sim\phi^{1/2}$).
(c) The variation of the diffusive absorption lengths with volume filling factor in $K_5Bi_{0.9}Nd_{0.1}(MoO_4)_4$ laser crystal powders has been studied. We have experimentally demonstrated that the diffusive absorption length depends inversely on the volume filling factor, indicating that the assumption of independent scattering made in these 'closely packed' crystal powders can be considered correct.

Acknowledgments

This work was supported by the Spanish Government MEC (MAT2004-03780) and the Basque Country University (UPV13525/2001). The authors would like to thank Dr Sergio Fernández Armas (Servicio General de Microscopía Electrónica y Microanálisis de Materiales Universidad del País Vasco) for performing the scanning electron microscope photographs.

Appendix

The *scattering mean-free-path* l_s, is the length of the light path in which intensity is reduced to $1/e$ of its initial value due to scattering. It is also defined as the average distance between two successive scattering events. The *transport mean-free-path* l_t, is defined as the average distance the light travels before its direction of propagation is randomized. The *inelastic mean-free-path* l_i, is the length of the light path in which intensity is reduced to $1/e$ of its initial

value due to absorption. The *diffusive absorption length* l_{abs}, is defined as the average distance between the beginning and the end points of paths of length l_{i}, $l_{\mathrm{abs}} = \sqrt{\frac{l_{\mathrm{t}} l_{\mathrm{i}}}{3}}$. l^* is the *extinction mean-free-path* $l^* = (\frac{1}{l_{\mathrm{i}}} + \frac{1}{l_{\mathrm{s}}})^{-1}$.

References

[1] Markushev V M, Zolin V F and Briskina C M 1986 *Sov. J. Quantum. Electron.* **16** 281
[2] Gouedard C, Husson D, Sautert C, Auzel F and Mignus A 1993 *J. Opt. Soc. Am.* B **10** 2358
[3] Noginov M A, Noginova N E, Caulfield H J, Venkateswarlu P, Thompson T, Mahdi M and Ostroumov V 1996 *J. Opt. Soc. Am.* B **13** 2024
[4] Wiersma D S and Lavendijk A 1996 *Phys. Rev.* E **54** 4254
[5] Soest G S, Poelwijk F J, Sprik R and Lagendijk A 2001 *Phys. Rev. Lett.* **86** 1522
[6] Noginov M A *et al* 2006 *J. Opt. A: Pure Appl. Opt.* **8** 285
[7] van der Molen K L, Tjerkstra R W, Mosk A P and Lagendijk A 2007 *Phys. Rev. Lett.* **98** 143901
[8] Noginov M A 2005 *Solid-State Random Lasers* (New York: Optical Sciences Springer)
[9] Nostrand M C *et al* 2001 *J. Opt. Soc. Am.* B **18** 264
[10] Jenkins N W, Bowman S R, Shaw L B and Lindle J R 2002 *J. Lumin.* **97** 127
[11] Mendioroz A, Balda R, Voda M, Al-Saleh M and Fernández J 2004 *Opt. Mater.* **26** 351
[12] Kaminskii A A, Sarkisov S E, Bohm J, Reiche P, Schultze D and Uecker R 1977 *Phys. Status Solidi* a **43** 71
[13] Voda M, Iparraguire I, Fernández J, Balda R, Al-Saleh M, Mendioroz A, Lobera G, Cano M, Sanz M and Azkargorta J 2001 *Opt. Mater.* **16** 227
[14] Iparraguirre I, Balda R, Voda M, Al-Saleh M and Fernández J 2002 *J. Opt. Soc. Am.* B **19** 2911
[15] Fernández J, Iparraguirre I, Aramburu I, Illarramendi M A, Azkargorta J, Voda M and Balda R 2003 *Opt. Lett.* **28** 1341
[16] Kurtz S K and Perry T T 1968 *J. Appl. Phys.* **39** 3798
[17] Jerphagnon J and Kurtz S K 1970 *Phys. Rev.* B **1** 1739
[18] Noginov M A, Zhu G, Frantz A A, Novak J, Williams S N and Fowlkes I 2004 *J. Opt. Soc. Am.* B **21** 191
[19] Totsuka K, Soest G S, Ito T, Lagendij A and Tomita M 2000 *J. Appl. Phys.* **87** 7623
[20] Ling Y, Cao H, Burin A L, Ratner M A, Liu X and Chang R P 2001 *Phys. Rev.* A **64** 063808
[21] Voda M, Al-Saleh M, Lobera G, Balda R and Fernández J 2004 *Opt. Mater.* **26** 359
[22] Genack A Z and Drake J M 1990 *Europhys. Lett.* **11** 331
[23] Garcia N, Genack A Z and Lisyansky A A 1992 *Phys. Rev.* B **46** 14475
[24] Gomez-Rivas J, Sprik R, Soukoulis C M, Busch K and Lagendijk A 1999 *Europhys. Lett.* **48** 22
[25] Gómez Rivas J 2002 Light in strongly scattering semiconductors; diffuse transport and Anderson localization *Thesis* University of Amsterdam
[26] Illarramendi M A, Aramburu I, Fernández J, Balda R, Williams S N, Adegoke J A and Noginov M A 2007 *J. Opt. Soc. Am.* B **24** 43
[27] Zhu J X, Pine D J and Weitz D A 1991 *Phys. Rev.* A **44** 3948
[28] Bohren C F and Huffman D R 1983 *Absorption and Scattering of Light by Small Particles* (New York: Wiley)
[29] Illarramendi M A, Aramburu I, Fernández J, Balda R and Al-Saleh M 2007 *J. Phys.: Condens. Matter* **19** 36206